Boron deficiency-induced changes in the subcellular composition and anatomical structure of petiole rings hinder nutrient transport in cotton (Gossypium hirsutum)

Mingfeng Li
wei Zhang
zhuqing Zhao
Xinwei Liu (lxw2016@mail.hzau.edu.cn)
Huazhong Agriculture University https://orcid.org/0000-0001-7997-5465

Research Article

Keywords: boron deficiency, cell wall, transport, vessels, cotton, petiole ring,

Posted Date: April 18th, 2022

DOI: https://doi.org/10.21203/rs.3.rs-1512263/v1

Boron deficiency-induced changes in the subcellular composition and anatomical structure of petiole rings hinder nutrient transport in cotton (*Gossypium hirsutum*)

Authors:

Mingfeng Li[a,b], Zhangwei[a,c], Zhuqing Zhao[a,c], Xinwei Liu[a,c*]

Affiliations:

[a] *Microelement Research Center, Huazhong Agricultural University, Wuhan 430070, China*

b Wuhan University of Bioengineering, Wuhan 430070, China

[c]*Hubei Provincial Engineering Laboratory for New-Type Fertilizer, Wuhan 430070, China*

Email addresses： mingfengL0124@163.com (M. Li), zzq@mail.hzau.edu.cn (Z. Zhao),

***Correspondence author:** Xinwei Liu (e-mail: lxw2016@mail.hzau.edu.cn, Tel: +86-027-87282137, Fax: 86-027-87282145)

Postal address: College of Resources and Environment, Huazhong Agricultural University No.1, Shizishan Street, Hongshan District, Wuhan, Hubei Province, 430070, PR. China

ABSTRACT

Background and aims The formation of brown rings on leaf petioles is a typical symptom of early boron deficiency in cotton. The purpose of this study was to examine the developmental defects of cell walls and vessels at the ring sites of cotton petioles and thereby understand the effects of petiole rings on nutrient transport in cotton.

Methods Boric acid (H_3BO_3, 13.5 kg B ha^{-1}) was applied as basal fertilizer in boron-deficient cotton field to verify the relationship between boron concentration and ring formation on cotton petioles. Petiole samples were taken from boron-deficient cotton plants 60 days post-transplantation to analyze the differences in cell wall properties and anatomical structure between the ring and non-ring sites. The transport of mineral nutrients in the upper, middle, and lower parts of the petioles was analyzed.

Results Under boron deficiency stress, chloroplasts were deformed and slightly disintegrated at the ring sites of the petioles. The cell walls within the rings were irregularly thickened by 44.1%, while their mechanical strength was markedly reduced by 38.9% compared to those of the non-ring sites. There were also changes in the hydrogen bonding within carbohydrates and proteins and the structure of pectins along with cellulose accumulation in the cell walls at the ring sites. A large number of tiny vessels were formed in the petiole rings, resulting in the squeezing and rupture of vessels. Boron, magnesium, and manganese concentrations in various parts of the petioles varied substantially in the order of lower part > middle part > upper part.

Conclusions Boron application reduces the probability of ring formation on the petioles of cotton. The cell walls and vessels are destructed at the ring sites of the petioles, which impairs their mechanical support and mineral nutrient transport functions in boron-deficient cotton.

Keywords: boron deficiency; cell wall; transport; vessels; cotton; petiole ring；

1 Introduction

Boron is an essential micronutrient for vascular plants, and boron deficiency is a serious

agricultural problem worldwide (Matthes et al., 2020). In order to improve resistance to boron deficiency, the plants alter their morphology through modulation of physiological and developmental responses. Therefore, boron deficiency induces various physiological symptoms in the plants, including the inhibition of root elongation, young leaf expansion, stem cracking, flower formation, and seed germination (Uraguchi and Fujiwara., 2011; Hua et al., 2016; Wu et al., 2018; Milagres et al., 2019; Matthes et al., 2020).

Cotton (*Gossypium hirsutum*) is a fibrous plant of the genus *Gossypium* in the family Malvaceae. Cotton fiber provides the raw materials for textile, while cotton seeds are rich in protein and fat, and thus can be used as an important oil and feed material (Bellaloui et al. 2015). Boron is considered to be the most deficient micronutrient in cotton and it is also a major limiting factor for cotton yield improvement (Ahmad et al., 2009). In the Yangtze River Basin, one of the three major cotton-producing areas in China, the soil is severely deficient in boron with the available boron concentration of only 0.33 mg kg^{-1} (Wang *et al*., 1989). Generally, plant symptoms of boron deficiency depend on the deficiency level of this soil nutrient. Under mild stress of boron deficiency, brown rings separated from each other appear on cotton petioles. Under severe stress of boron deficiency, the rings protrude outwardly and crack on the exterior surface of the petioles; cotton plants form buds without flowering, and the plant type is compact and short, even leading to complete crop failure (Wang et al., 1989; Zhao and Oosterhuis., 2002; Abid et al., 2007; Li et al., 2017). Wang et al. (1985) have shown that the probability of ring formation on cotton petioles is negatively correlated with the available boron concentration in the soil. In the case of mild boron deficiency, brown rings appear on the exterior surface of cotton petioles. Because this symptom is clear and distinct, it can be used as the primary diagnostic marker of early boron deficiency in cotton.

The petiole is a vital organ for mechanical support and nutrient transport in cotton. Especially due to the function of vascular bundles in transport of plant nutrients, water, organics, and hormones, petioles play an essential role in the physiological metabolism of cotton. Boron is crucial for the development of vascular tissues in many dicotyledonous plant taxa and boron deficiency particularly affects the integrity of phloem and xylem vessels, and, therefore, functionality of long-distance transport (Pommerrenig et al., 2019). However, the

research on petiole rings formed in boron-deficient cotton is currently in a stagnant state. The effects of petiole rings on cotton growth and development merit further exploration, and the differences between the ring and non-ring sites of cotton petioles needs to be thoroughly investigated. Microscopic observation of plant tissues following dissection provides an approach to directly examine the changes in plant morphology and structure. Previous studies have mainly observed boron deficiency-induced changes in the anatomical structure of plant leaves and roots (Li et al., 2016; Mesquita., 2016; Muhammad et al., 2018). However, there remains no detailed comparison of the anatomical structure of petioles between the ring and non-ring sites in cotton under boron deficiency stress.

In this study, we directly observed the ring and non-ring sites of boron-deficient cotton petioles by sectioning of paraffin-embedder tissue, scanning electron microscopy (SEM), transmission electron microscopy (TEM), and Fourier-transform infrared spectroscopy (FTIR) based on field experiment. The objectives of the study were to clarify: (1) the structural changes in cell walls and vessels at the ring sites of cotton petioles, and (2) the effects of petiole rings on mineral nutrient transport in cotton under boron deficiency stress.

2. Materials and methods

2.1 Experimental site and materials

The field experiment was conducted in Shaling Village, Tianmen City, Hubei Province, China. The soil type in the experimental site was calcareous alluvial soil with a pH of 7.53. The experimental soil contained: organic matter, 19.58 g kg^{-1}; alkali-hydrolyzale nitrogen, 66.38 mg kg^{-1}; available phosphorus, 6.15 mg kg^{-1}; available potassium, 68.14 mg kg^{-1}; and available boron, 0.23 mg kg^{-1}.

Seeds of cotton were *Gossypium hirsutum* cv. 'Jinxiu-88'. Fertilizers were applied at rates of 375 kg N ha^{-1} in the form of urea (46% N), 144 kg K_2O ha^{-1} in the form of chloride potassium (60%, K_2O), and 73.5 kg P_2O_5 ha^{-1} in the form of calcium superphosphate (14% P_2O_5). The planting density was 25,000 plants ha^{-1}.

2.2 Experimental treatment, sample preparation, and analysis methods

Experimental treatment: Two different levels of boron (as H_3BO_3) were applied: 0 kg B ha^{-1} (boron deficiency, B0) and 13.5 kg B ha^{-1} (boron sufficiency, B13.5). The plot area was

72 m^2, with four replications per treatment. Leaf and petiole samples were taken from the fourth expanded leaf from the apex of cotton plants 60 days post-transplantation. Specifically, we analyzed the petioles from boron deficiency treatment (B0): **the ring sites versus the non-ring sites (Fig. 1)**. A portion of the petiole samples were divided into ring and non-ring sites for tissue section preparation and cell wall extraction. The other portion of the petiole samples was separated into upper, middle, and lower parts; each part was deactivated at 105°C for 30 min and dried at 65°C to constant weight, then ground and sealed in plastic bags until mineral nutrient analysis.

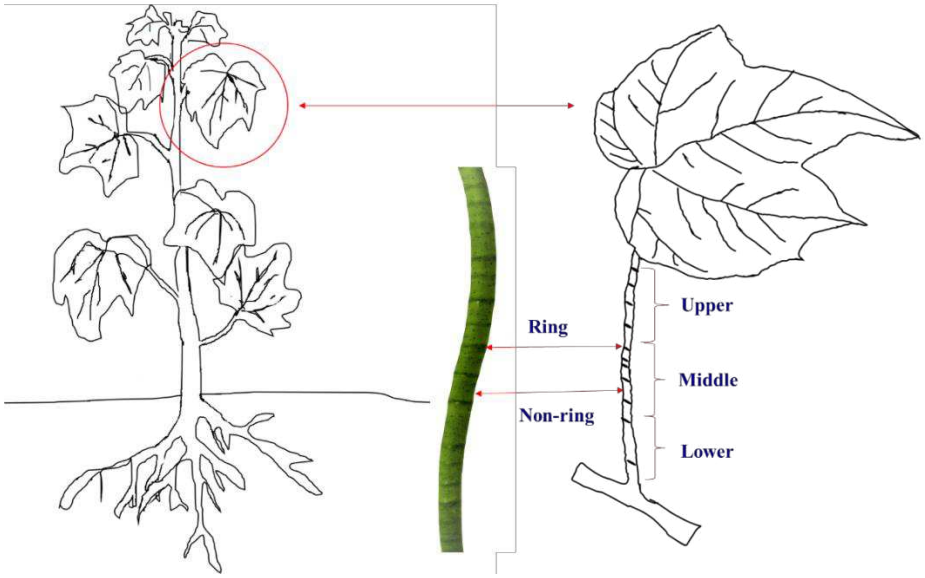

Fig. 1 The sampling sites of cotton petiole

SEM observation: Petiole samples of the ring and non-ring sites were rinsed with deionized water and cut longitudinally. The samples were washed with 0.1 mol L^{-1} phosphate-buffered saline (PBS; pH = 7.4) and then fixed with glutaric acid for 12 hours. Afterwards, the samples were rinsed with PBS (pH = 7.4) and then fixed with 1% osmium tetraoxide for 0.5 hours. Following three rinses with PBS (pH = 7.4), the samples were successively dehydrated in different concentrations (50%, 70%, 80%,95% and 100%) of ethanol for 15 min. Subsequently, the samples were added with isoamyl acetate and incubated for 10–20 min, followed by drying in a critical point dryer. The tissue blocks were fixed on the sample stage and sprayed with coat using a JFC-1600 ion sputter (JEOL, Tokyo, Japan).

Finally, the samples were observed and photographed under a JSM-6390LV scanning electron microscope (JEOL).

TEM observation: Petiole samples of the ring and non-ring sites were rinsed with deionized water and cut longitudinally. TEM sections were prepared using the method of Kong et al. (2013). The tissue samples were sliced (50-60 nm) using an ultra-thin microtome. After staining with 2% uranyl acetate and lead citrate the sections were observed and photographed under a transmission electron microscope. Cell wall thickness was measured using the "Ruler" tool in Adobe Photoshop CS6.

Fluorescence microscopy observation: Paraffin-embedded tissue sections were prepared using the method described by Li et al. (2016). After safranin O and fast green staining, the sections were dried in a 60°C oven followed by dehydration and clarification with xylene. Finally, the sections were dried and mounted with neutral gum. The prepared sections were observed and photographed under an Eclipse Ci fluorescence microscope (Nikon, Tokyo, Japan). Vascular bundle related indicators were measured using Image-Pro Plus 6.0 (Media Cybernetics Inc., Rockville, MD, USA).

Vessel isolation and size measurement: The separation of vessel elements was performed using the chromic acid/nitric acid isolation method (Li et al., 2016). Briefly, petiole samples of the ring and non-ring sites were repeatedly boiled twice in water until all the samples sank to the bottom. The boiled water was poured and 10% chromic acid solution was added for 2 hours of dispersion. The dispersed samples were stained with 1% safranin O solution for 15 min. After removal of the excess staining solution, each sample was cut into eight temporary sections. The sections were observed under a BX61 light microscope, with 10 fields of view selected at random for each section. A total of 80 fields of view were observed per treatment. The types of vessels were examined and counted. Vessel diameter and length were measured using Image-Pro Plus 6.0 (Media Cybernetics Inc.).

Cell wall extraction: Cell wall components of cotton petioles were extracted using the method of Hu and Brown (1994). Briefly, fresh samples (each 5.**** g) of the ring and non-ring sites were ground in liquid nitrogen and the homogenates were transferred into 10 volumes of 4°C pre-cold ultrapure water. After centrifugation (1000g, 10 min), the

supernatants were discarded and the residues were rinsed with 10 volume of pre-cold water. The centrifugation procedure was repeated three times. Subsequently, the residues were rinsed three times with 10 volumes of 80% ethanol, and then rinsed once with 10 volumes of methanol–chloroform mixture (1:1, v/v) followed by 10 volumes of acetone. The remaining insoluble residues were collected as crude cell walls and dried in a 105℃ oven.

Cell wall mechanical analysis by atomic force microscopy (AFM): The mechanical properties of petiole cell walls were analyzed using the method of He et al. (2015). Briefly, the crude cell walls were re-suspended in ultrapure water for 1 hour. The suspensions were dropped on clean glass slides with a pipette and air-dried overnight. AFM imaging was performed using an atomic force microscope (Bruker, Santa Barbara, CA, USA) in the ScanAsyst-Air mode. Images were captured using Bruker Scan Asyst-Air probes with a tip radius of 2–12 nm and silicon nitride cantilever (spring constant, 0.4 N m^{-1}). All images were acquired at a low scanning speed of 1 Hz and quantitatively analyzed using the Nano Scope Analysis software (Bruker). For quantitative mechanical analysis with AFM, the deflection sensitivity (30-35 nm V^{-1}) and precise spring constant (30–60 N m^{-1}) of each probe used were corrected using the AFM system software before sample measurement (He et al., 2015). The Young's modulus was obtained by calculation based on the Hertz model using the Nano Scope analysis software (Bruker), and the Poisson's ratio of the samples was set to 0.3.

FTIR analysis of cell wall composition: The crude cell walls were oven-dried, ground, and passed through a 100-mesh sieve. An appropriate amount of cell wall powder was thoroughly mixed with potassium bromide (1:100, w/w) in an agate mortar. The mixture was ground and introduced into a hydraulic press (Graseby-Specac Press, UK) to fabricate uniform transparent tablets. Infrared spectra were acquired using a VERTEX 70 Fourier infrared spectrometer (Bruker) in the spectral range of 4000–400 cm^{-1} with a resolution of 4 cm^{-1}, and the scans were performed 32 times in total. The background was scanned before the measurement of each sample, and the obtained infrared spectra were used for baseline correction to ascertain the peak value and absorbance.

Mineral nutrient analysis: Total nitrogen and potassium concentrations in leaf and petiole samples were respectively determined by semi-micro Kjeldahl method and flame

photometry after digestion with H_2SO_4-H_2O_2. The boron, calcium, magnesium, and manganese concentrations were determined by inductively coupled plasma-mass spectrometry after digestion with HNO_3-H_2O_2 (4:1, v/v).

2.3. Statistical analysis

Data were statistically analyzed using SPSS Statistics v17.0 (SPSS Inc., Chicago, IL, USA). T test was used for multiple comparisons. A *P* value of less than 0.05 was considered to indicate significant differences between the treatments ($P < 0.05$).

3. Results

3.1. Effects of boron application on probability of petiole ring formation and boron concentration in cotton

We observed the formation of separated brown rings on the petioles of cotton plants grown under boron deficiency stress, but no rings appeared on the petioles of plants receiving sufficient boron fertilizer (Fig. 2, left). Following boron application, the probability of ring formation declined by 78.6% ($P < 0.05$; Fig. 2, right), while the boron concentrations in cotton leaves and petioles increased by 80.7% and 68.0%, respectively ($P < 0.05$; Fig. 3), as compared to those with no boron application. These results indicate that boron is a vital nutrient factor affecting the formation of petioles in cotton.

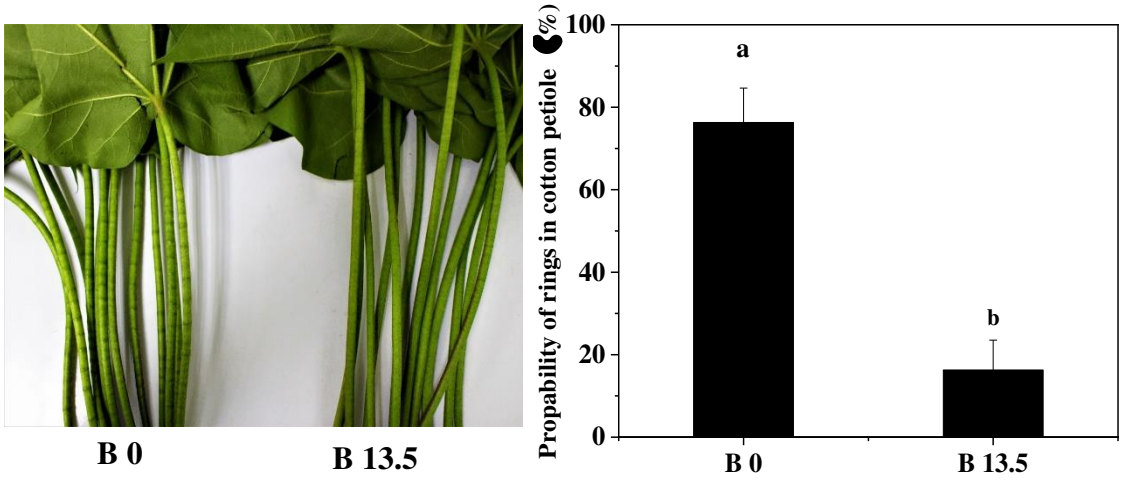

Fig. 2 Effects of boron application on formation of petiole rings in cotton. B0 represents boron deficiency treatment (0 kg B ha^{-1}) and B13.5 represents boron sufficiency treatment (13.5 kg B ha^{-1}). Data are the means of four replicates (± standard). Different lowercase letters above error bars indicate significant differences between the treatments ($P < 0.05$)

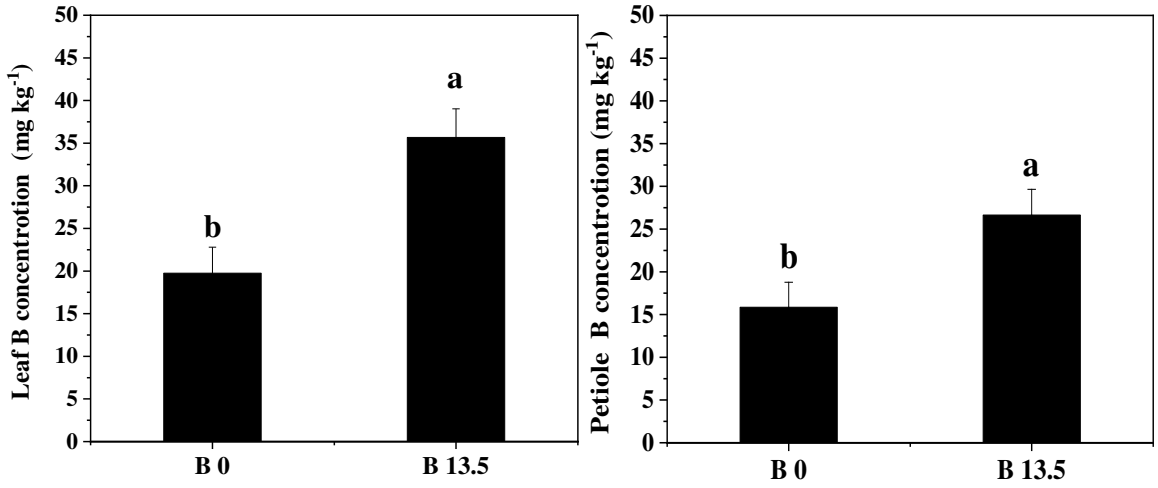

Fig. 3 Effects of boron application on boron concentrations in leaves and petioles of cotton. B0 represents boron deficiency treatment (0 kg B ha^{-1}) and B13.5 represents boron sufficiency treatment (13.5 kg B ha^{-1}). Data are the means of four replicates (± standard). Different lowercase letters above error bars indicate significant differences between the treatments ($P < 0.05$)

3.2. Changes in cell wall morphology and composition between ring and non-ring sites of cotton petioles

After ring formation, we divided the petioles from boron-deficient cotton plants into ring sites and non-ring sites according to their morphological changes (Fig. 1). SEM images show that at the ring sites, the cell walls were thickened irregularly, while the chloroplasts were long and thin, deformed and slightly disintegrated, with an increased number of starch granules (Fig. 4A, B).At the non-ring sites of the petioles, the organelles including chloroplasts and mitochondria were generally complete; the cell wall thickness was relatively uniform and the chloroplasts had a full fusiform shape (Fig. 4C, D). The mean cell wall thickness at the ring sites was 1.44-fold that at the non-ring sites of the petioles (Fig. 4E).

We obtained the force-distance curve by pressing the AFM probe into the cell wall surface and then transformed it into Young's modulus to characterize the mechanical strength of petiole cell walls (Fig. 4F). Young's modulus of the cell walls at the non-ring sites was 4.96 Gpa. Following ring formation, Young's modulus of the cell walls changed to 3.03 Gpa. The decrease in Young's modulus of petiole cell walls at the ring sites is indicative of a decline in cell wall stability.

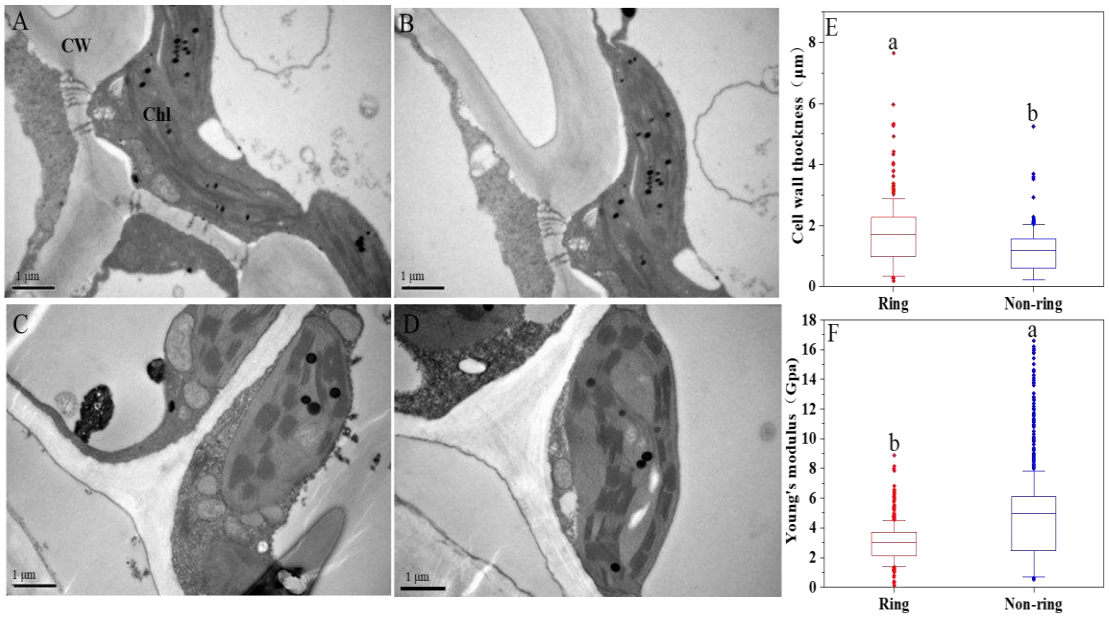

Fig. 4 Differences in cell wall morphology and mechanical strength between ring and non-ring sites of cotton petiole. A, B: ring subcellular structure; C, D: non-ring subcellular structure; E: cell wall thickness; and F: Young's modulus. CW: cell wall; Chl: chlorophyll. The horizontal line of each box represents the mean value; the whiskers outside the box extend to the 5% and 95% percentiles; and scatters represent outliers

We used FTIR spectra to distinguish the functional groups present in petiole cell walls and to identify the chemical composition of the cell walls at the ring and non-ring sites. Substantial differences were observed between the ring and non-ring sites of cotton petioles with regard to the position and relative absorbance of the peaks in the wavenumber range of 4000–800 cm^{-1} (Fig. 5). A characteristic absorption peak was observed at around 3400 cm^{-1}, which is attributed to the stretching vibration of O-H and N-H in carbohydrates and proteins; this peak is therefore mainly derived from hydrogen bonds (Yang and Yen, 2002). Compared to that of the non-ring sites, the absorption peak of petiole cell walls at the ring sites shifted to high wavenumber by 15.5 cm^{-1} and its relative absorbance also increased, indicating that ring formation alters the hydrogen bonds within carbohydrates and proteins in the petiole cell wall.

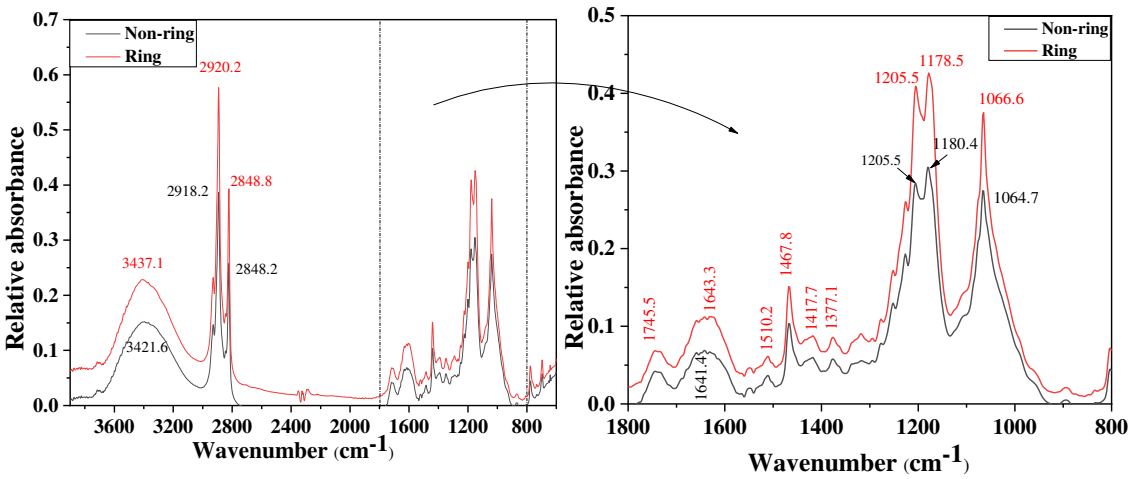

Fig. 5 Differences in Fourier-transform infrared spectra of petiole cell walls between ring and non-ring sites

The characteristic absorption peaks at around 2920 and 2850 cm^{-1} are attributed to the reverse stretching vibration of C-H, which is mainly derived from the wax and cellulose in the cell wall (Abidi et al. 2008). Compared to that of the non-ring sites, the relative absorbance of these two peaks of petiole cell walls at the ring sites increased, suggesting the accumulation of wax and cellulose. The absorption peak at around 1745 cm^{-1} is attributed to the stretching vibration of C=O from the ester group (-COOR) in cell wall pectins (Alonso-Simon et al., 2011). The cell wall strength increased in the petiole rings, indicating structural changes in cell wall pectins after ring formation.

The absorption peaks at around 1640 and 1510 cm^{-1} are attributed to amide I and amide II absorption bands of cell wall protein (Tatulian 2013). Compared to those of the non-ring sites, the two peaks of petiole cell walls at the ring sites had enhanced absorption intensity, indicating the destruction of protein structure in the petiole cell wall by the rings. Moreover, the absorption peak at around 1060 cm^{-1} mainly indicates different vibration modes of the polysaccharide skeleton (Barron et al. 2005). The absorption intensity of this peak was also enhanced at the ring sites compared to the non-ring sites. Altogether, the results indicate that there are changes in the content and structure of cell wall components after the formation of petiole rings.

3.3. Changes in anatomical structure between ring and non-ring sites of cotton petioles

Fluorescence microscopy observation revealed that the petioles of cotton were comprised

of epidermis, cortex, vascular bundles, and pith cells (Fig. 6). At the non-ring sites, there was a relatively long distance between the epidermis and vascular bundles; phloem and xylem cells were arranged in an orderly manner, while pith cells were characterized by a neat, compact arrangement and a large size. Comparing the ring sites to the non-ring sites, we observed an overgrowth of vascular bundles, along with 11.0%, 14.6% and 23.9% increases in the areas of vascular bundles, xylem, and phloem, respectively. The number of parenchyma cells between xylem vessels decreased, while the vessel area and number respectively increased by 15.8% and 28.3% at the ring sites compared to the no-ring sites. Additionally, there was an abnormal increase of pith cells which were deformed and squeezed at the ring sites (Fig. 6, Table 1).

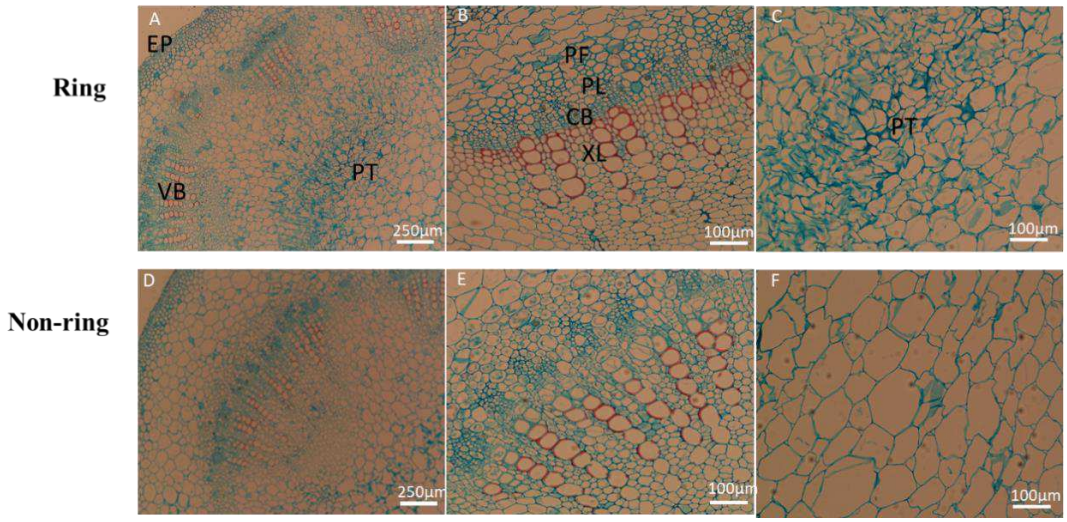

Fig. 6 Fluorescence microscopy observation on longitudinal paraffin-embedded sections of cotton petioles at ring and non-ring sites. A: ring, bar = 250 μm; B and C: ring, bar = 100 μm; D: non-ring, bar = 250 μm; E and F: non-ring, bar = 100 μm; EP: Epidermis; VB: vascular bundle; PT: pith; PF: phloem fiber; PL: phloem; CB: cambium; and XL: xylem

295 **Table 1** Changes in anatomical structure between ring and non-ring sites of cotton petiole

Sampling site	Cross-sectional area (mm^2)	Vascular bundle area (mm^2)	Xylem area (mm^2)	Phloem area (mm^2)	Vessel number (No.)	Vessel area (mm^2)
Ring	18.10±1.18a	4.53±0.35a	2.27±0.16a	1.09±0.17a	761±65a	0.88±0.07a
Non-ring	17.66±1.08a	4.08±0.28b	1.98±0.17b	0.88±0.12b	593±34b	0.76±0.05b

296 Note: Data are the means of eight replicates (± standard). Values with different lowercase
297 letters are significantly different between the sampling sites using the t-test ($n = 8$, $P < 0.05$)

298 To explore the effect of ring formation on the transport function of cotton petioles, we
299 further observed the morphology of vessel elements in the petioles by TEM. At the ring sites,
300 there was an overgrowth of vessels which were dry and deformed; a large number of
301 perforations occurred on the side wall of the vessels (Fig. 7A, C). At the non-ring sites, the
302 vessels were arranged in an orderly manner; the vessels were full and round with large
303 diameter and loose structure (Fig. 7B, D). A large number of tiny vessels appeared in the
304 petioles after ring formation, causing significant reductions in vessel diameter and length at
305 the ring sites (Fig. 8).

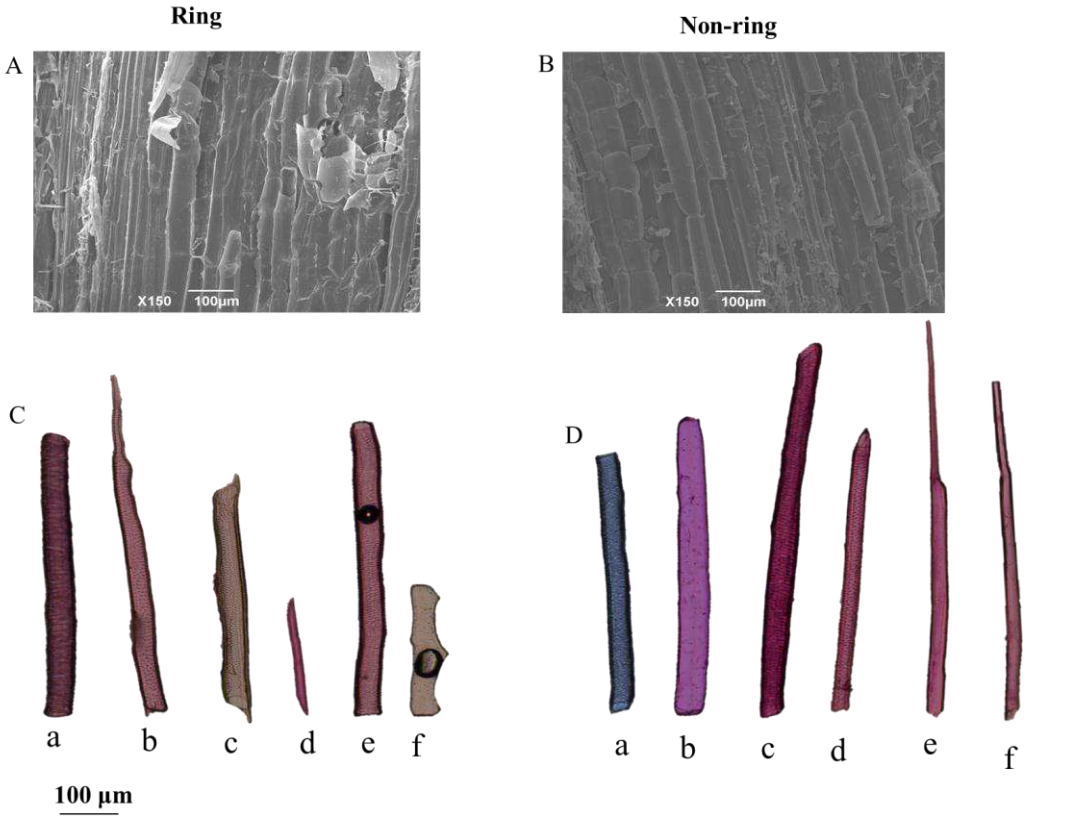

Fig. 7 Vessel morphologies in ring (A, C) and non-ring (B, D) sites of cotton petioles

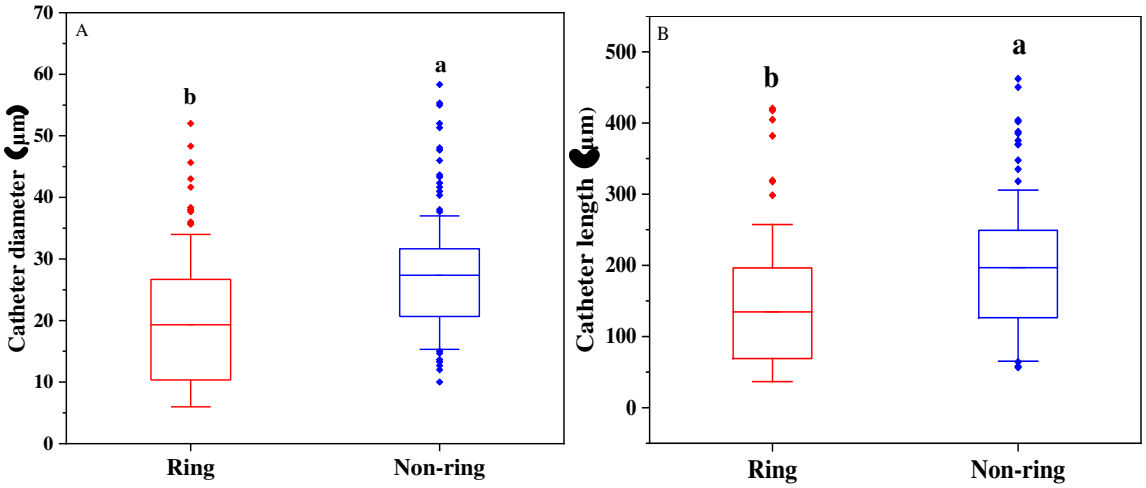

Fig. 8 Diameter (A) and length (B) of vessels at ring and non-ring sites of cotton petioles. The horizontal line of each box represents the mean value; the whiskers outside the box extend to the 5% and 95% percentiles; and scatters represent outliers.

3.4. Change in mineral nutrient concentrations in various parts of cotton petioles

To verify the effect of ring formation on mineral nutrient transport in cotton petioles, we divided the petioles of functional leaves from boron-deficient cotton plants into three parts. No significant changes were observed in the nitrogen, potassium, and calcium concentrations among the upper, middle, and lower parts of petioles after ring formation. However, the boron, magnesium, and manganese concentrations changed in the order of lower part > middle part > upper part. Specifically, the boron, magnesium, and manganese concentrations in the upper part of the petioles were 18.1%, 21.0% and 31.8% lower than those in the lower part, respectively ($P < 0.05$; Fig. 9). This result indicates that the formation of brown rings on the petioles hinders the transport of mineral nutrients from the roots to the leaves in boron-deficient cotton.

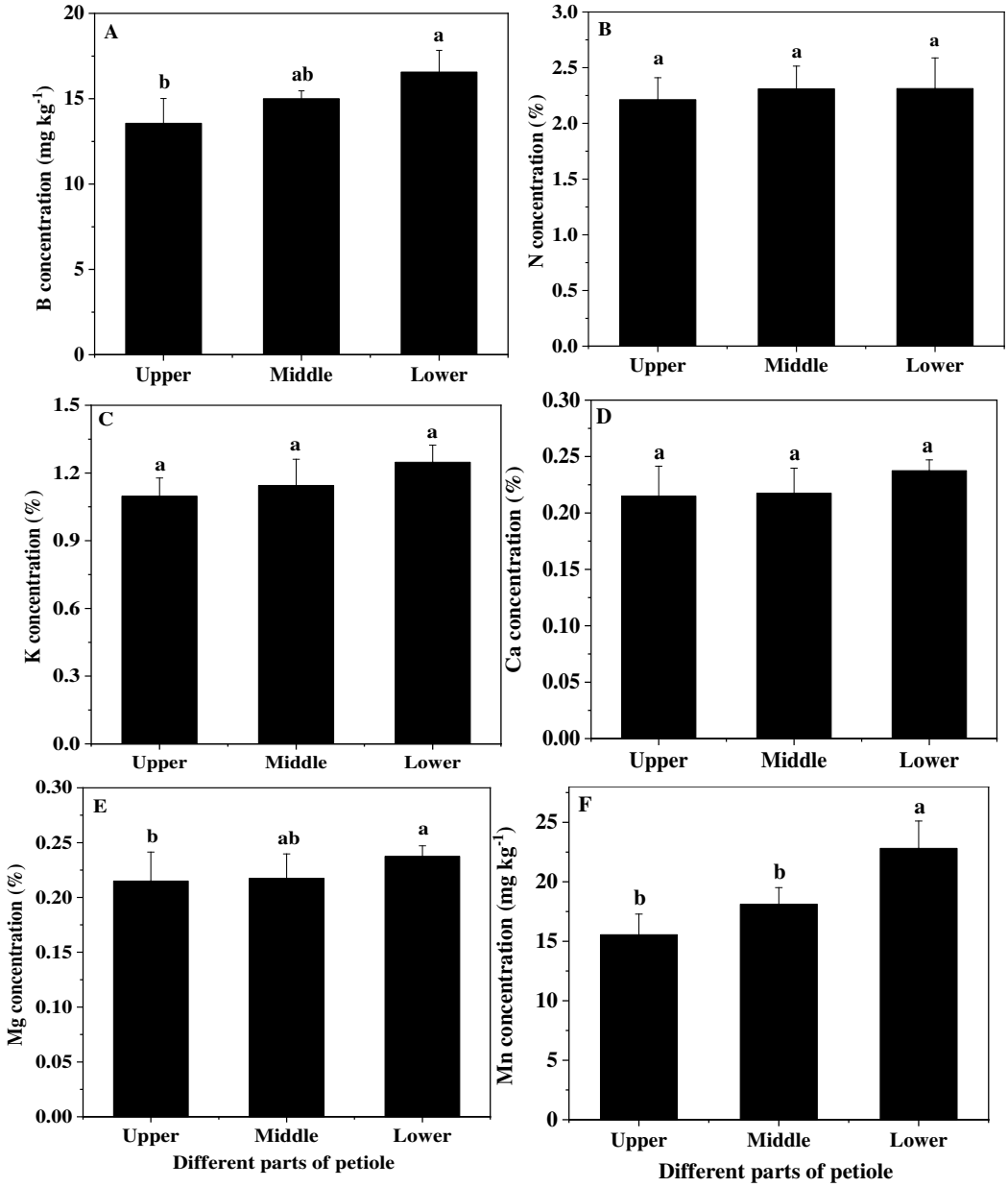

Fig. 9 Differences in boron (A), nitrogen (B), potassium (C), calcium (D), magnesium (E), and manganese (F) concentrations in various parts of boron-deficient cotton petioles. Data are the means of four replicates (± standard). Different lowercase letters above error bars indicate significant differences among the three parts of petioles ($P < 0.05$).

4. Discussion

During plant growth and development, different environments induce changes in the physiological and metabolic activities in various parts of the plants, which affects the construction of organs and tissues, thereby leading to differences in plant morphology. Under boron deficiency stress, rape (*Brassica napus* L.) is characterized by thin plants, curled leaves,

retarded growth, and cracked stems (Hua et al., 2016). Compared to healthy plants, boron-deficiency radish (*Raphanus sativus* L.) plants have smaller leaves that are unevenly thickened with curved edges (Cong et al., 2015). Here, our results indicate that boron deficiency induces the formation of brown rings on the petioles of cotton during the seedling stage; the application of boron fertilizer considerably increases boron concentrations in the petioles and leaves of cotton, thereby reducing the probability of ring formation. When subjected to boron deficiency stress, cotton plants exhibit curling of new leaves, blockage of apical growing point, and death of apical buds, along with flower and boll abscission during the development of reproductive organs (Bogiani et al., 2014; Wu et al., 2017). In short, brown rings formed on the petioles can be used as an indicative symptom of boron deficiency in cotton at the seedling stage.

The plant cell wall is a highly complex and dynamic structure composed of cellulose, hemicellulose, pectin, lignin, protein, and inorganic molecules (Showalter et al., 1996). Boron deficiency stress results in the thickening of plant cell walls, which in turn destructs the internal structure of the cells, causing slight disintegration and even disappearance of various organelles within the cells (Shah et al., 2017). In the present study, we demonstrated an inconsistency in the composition and structure of petiole cell walls between the ring and non-ring sites in cotton plants under mild boron deficiency stress (Figs. 4 and 5). Particularly, the relative absorbance of the peaks attributed to wax and cellulose was increased in the petiole rings (Fig. 5), indicating more cellulose accumulation occurring in petiole cell walls. According to Hu and Brown (1994), higher levels of cellulose hinder the extension and structural changes of plant cell walls, thereby leading to cell wall thickening. This could explain our observation that petiole cell walls were irregularly thickened at the ring sites compared to the non-ring sites in boron-deficient cotton (Fig. 4).

Cong et al. (2015) indicated that boron deficiency reduces the bonding between pectic polysaccharides and plant cell walls, thereby decreasing cell wall plasticity and easily causing the cell walls to rupture. In the current study, the results showed that the mechanical strength of petiole cell walls was reduced at the ring sites compared to the non-ring sites in cotton plants under boron deficiency stress, which decreased cell wall stability (Fig. 4). The

absorption of the peak attributed to the ester group (-COOR) in pectins was increased in the petiole rings, indicating structural changes in cell wall pectins after ring formation on cotton petioles. Moreover, the hydrogen bonding between protein and polysaccharide molecules was destructed at the ring sites, which inevitably impaired the integrity and function of petioles cell walls. In short, the composition and structure of plant cell walls are inconsistent between the ring and non-ring sites in cotton under boron deficiency stress. Especially, the normal structure and function of petiole cell walls are impaired in the rings, which in turn affects the transport function of the petioles.

Liu et al. (2013) observed that boron deficiency causes an overgrowth of vascular bundles in the leaf veins of citrus (*Citrus reticulata* Blanco), with leaf vein burst in severe cases. Notably, we observed that boron deficiency-induced changes in cotton petioles were not uniform or continuous, which could be divided into alternately arranged ring and non-ring sites with substantial differences in their appearance (Fig. 2). Li et al. (2017) showed that there is continuous growth of vascular bundles in the petioles of cotton under boron deficiency stress; the vascular cambium is irregularly thickened, which extends to produce phloem outwardly and xylem inwardly. To further explore the nutrient transport changes in cotton petioles after ring formation, we performed an anatomical observation on the different sites of boron-deficient cotton petioles. We observed an orderly arrangement of phloem and xylem cells at the non-ring sites, with large pith cells arranged in an orderly and compact manner. At the ring sites, there was an overgrowth of vascular bundles, with pith cells increased abnormally, deformed and squeezed. Ishii et al. (2001) found that the sieve pores of vascular bundles are blocked after boron deficiency, resulting in callose and carbohydrate accumulation in the sieve tubes.

Xylem vessels are required for the continuous supply of water to the leaves to maintain photosynthesis and provide essential nutrient elements to the shoots (Wimmer and Eichert, 2013). Here, we observed numerous tiny vessels present in the petiole rings of boron-deficient cotton, which led to substantial reductions in vessel diameter and length compared to those at the non-ring sites (Fig. 6). Li (2012) showed that boron-deficient citrus plants have small-diameter vessels in leaf veins, with a large number of vessels per unit area

and low proportions of cavities and emboli; the vessels have high anti-pressure ability and are unlikely to collapse completely, but there exists large transport resistance with low transport efficiency. In the present study, the results showed that boron, magnesium, and manganese concentrations decreased remarkably from the lower part to the upper part of boron-deficient cotton petioles. This provides evidence that the formation of petiole rings hinders the migration of nutrient ions from the stems to the leaves of cotton. Li et al. (2016) found that boron deficiency induces side-wall perforations of vessels in the roots of citrus. Similarly, we also observed side-walls perforations of vessels in the petiole rings of boron-deficient cotton (Fig. 5C), which is favorable for the lateral transport of nutrients and water. In summary, a large number of tiny vessels are formed in the petiole rings, which is a self-rescue action for cotton to adapt to boron deficiency stress; however, many vessels are squeezed and collapsed, thus reducing the transport capacity of cotton petioles.

5 Conclusions

The formation of brown rings on cotton petioles is a typical symptom of mild boron deficiency. Under boron deficiency stress, the cell wall composition of cotton petioles is changed, along with cellulose accumulation. The cell walls are thickened irregularly and their mechanical strength is reduced. The vessels are prone to rupture and deformation. Consequently, the functionality of petioles declines in boron-deficient cotton. In order to adapt to boron deficiency stress, the plants form a large number of tiny vessels in the petiole rings, which reduces the rate of vessel embolization. The transport efficiency of the vessels is improved via side-wall perforations. However, many vessels are squeezed and deformed, with high transport resistance and thus low efficiency. Therefore, the presence of rings on the petioles reduces the transport of mineral nutrients from the root to the leaves in boron-deficient cotton.

Acknowledgements

The authors gratefully thank for the partially support by the Fundamental Research Funds for the Central Universities (2662018PY002).

contribution

xinwei Liu and zhuqing Zhao planned and designed the research.

mingfengLi and wei Zhang performed experiments, conducted fieldwork, analysed data etc.

mingfengLi wrote the manuscript

Standard Templates for Author Use

The data that support the findings of this study are openly available in [repository name e.g “figshare”] at http://doi.org/[doi], reference number [reference number].

References

Abid M, Ahmad N, Ali A, Chaudhry M, Hussain J (2007). Influence of soil–applied boron on yield, fiber quality and leaf boron contents of cotton (*Gossypium hirsutum* L.). J Agric Soc Sci 3, 7-10.

Abidi N. Hequet E, Cabrales L, Gannaway J, Wilkins T, Wells L (2008). Evaluating cell wall structure and composition of developing cotton fibers using Fourier transform infrared spectroscopy and thermogravimetric analysis. J Appl Polymer Sci 107, 476-486.

Ahmad S, Akhtar L, Iqbal N, Nasim M (2009). Short Communication Cotton (Gossypium hirsutum L.) varieties responded differently to foliar applied boron in terms of quality and yield. Soil Environ 28, 88-92.

Alonso-Simon A, Garcia-Angulo P, Melida H, Encina A, Alvarez J, Acebes J (2011). The use of FTIR spectroscopy to monitor modifications in plant cell wall architecture caused by cellulose biosynthesis inhibitors. Plant Signal. Behav 6,1104-1110

Barron C, Parker M, Mills E, Rouau X, Wilson R (2005). FTIR imaging of wheat endosperm cell walls in situ reveals compositional and architectural heterogeneity related to grain

hardness. Planta 220, 667-677.

Bellaloui N, Turley R, Stetina S (2015). Water Stress and Foliar Boron Application Altered Cell Wall Boron and Seed Nutrition in Near-Isogenic Cotton Lines Expressing Fuzzy and Fuzzless Seed Phenotypes. Plos One 10, e0130759.

Bogiani J, Sampaio T, Abreu-Junior C, Ciro A (2014). Boron uptake and translocation in cotton cultivars. Plant Soil 375, 241-253.

Cong X, Jing H, Lin N, Xia Z, Huang M, Jiang X (2015). Boron deficiency affects cell morphology and structure of young leaves of radish. Acta Physiol Plant 37,247.

He C, Ma J, Wang L (2015). A hemicellulose-bound form of silicon with potential to improve the mechanical properties and regeneration of the cell wall of rice. New Phytol 206,1051-1062.

Hu H, Brown P (1994). Localization of boron in cell walls of squash and tobacco and its association with pectin. Evidence for a structural role of boron in the cell wall. Plant Physiol 105, 681-689.

Hua Y, Zhou T, Ding G, Yang Q, Shi L, Xu F (2016). Physiological, genomic and transcriptional diversity in responses to boron deficiency in rapeseed genotypes. J Exp Bot 67, 5769-5784.

Ishii T, Matsunaga T, Hayashi N (2001) .Formation of rhamnogalacturonan IIborate dimer in pectin determines cell wall thickness of pumpkin tissue. Plant Physiol 126, 1698-1705.

Kong Y, Xu X, Zhu L (2013) Cyanbactericidal effect of Streptomyces sp. HJC-D1 on microcystis auruginosa. Plos One. 8, e57654.

Li M, Li Q, Wang H, Ou S, Shuang P (2016). Boron deficiency affects root vessel anatomy and mineral nutrient allocation of poncirus trifoliata (L.) raf. Acta Physiol Plant. 38, 1-8.

Li S, Peng S, Liu Y, Zhou G, Yang C (2012). Observations on morphological abnormalities of the vessel elements of veins and fruit of under boron deficiency. Plant Sci J 30,624-630.

Li M, Zhao Z, Zhang Z, Zhang W, Zhou J, Xu F, Liu X (2017). Effect of boron deficiency on anatomical structure and chemical composition of petioles and photosynthesis of leaves in cotton (*Gossypium hirsutum* L.). Sci rep-UK **7**, 1-9.

Liu Y, Li E, Yang C, Peng S (2013) Effects of boron-deficiency on anatomical structures in the leaf main vein and fruit mesocarp of pummelo [*citrus grandis* (L.) osbeck]. J Pomol Hor Sci 88, 693-700.

Matthes M, Robil J, McSteen P (2020) From Element to Development: The power of the essential micronutrient boron to shape morphological processes in plants. Journal of Exp Bot 42.

Mesquita G, Zambrosi C, Tanaka A, Boaretto M, Quaggio J, Ribeiro R V, Mattos Jr (2016) Anatomical and physiological responses of citrus trees to varying boron availability are dependent on rootstock. Front Plant Sci **7**, 224.

Milagres C, Maia J, Ventrella M, Martinez H (2019) Anatomical changes in cherry tomato plants caused by boron deficiency. Braz J Bot 42, 319–328

Muhammad R, Yan L, Wu X, Saddam H, Omar A, Jian C (2018) Boron deprivation induced inhibition of root elongation is provoked by oxidative damage, root injuries and changes in cell wall structure. Environ Exp Bot 18, 7.

Pommerrenig B, Eggert K, Bienert G (2019) Boron Deficiency Effects on Sugar, Ionome, and Phytohormone Profiles of Vascular and Non-Vascular Leaf Tissues of Common Plantain (*Plantago major* L.). In J Mol Sci 20, 3882.

Shah A, Wu X, Ullah A, Fahad S, Muhammad R, Yan L, Jiang C (2017) Deficiency and toxicity of boron: alterations in growth, oxidative damage and uptake by citrange orange

plants. Ecotox Environ Safe 145, 575-582.

Showalter A, Kieliszewski M, Cheung A, Tierney M (1996) Genes encoding cell wall proteins. Plant Mol Biol Report 14, 9-10.

Tatulian S (2013) Structural Characterization of Membrane Proteins and Peptides by FTIR and ATR-FTIR Spectroscopy Lipid-Protein Interactions. Method Mol Biol 974, 177-218.

Uraguchi S, Fujiwara T (2011) Significant contribution of boron stored in seeds to initial growth of rice seedlings. Plant Soil. 340, 435-442.

Wang Y, Liu W, Pi M, Wang Z (1989) B- deficiency in cotton and division of boron application in important producing cotton area of China. J Huazhong Agri Univ 8, 155-156.

Wang Y, Liu W, Pi M (1985) Study on the latent Boron Deficiency in Cotton and the Effective Application of Boron to Cotton. Sci Agri Sinica 18, 62-70.

Wimmer, M., Eichert T (2013) Review: mechanisms for boron deficiency-mediated changes in plant water relations. Int J Plant Sci. 203, 25-32.

Wu X, Dong X, Lu X, Riaz M, Jiang C (2017) Leaf structure and chemical compositions are correlated with cotton boron efficiency. J Plant Nutr 41, 552-562.

Wu X, Liu G, Riaz M, Lei Y, Jiang C (2018) Metabolic changes in roots of trifoliate orange [*poncirus trifoliate* (l.) raf.] as induced by different treatments of boron deficiency and resupply. Plant Soil 2, 1-13.

Yang J, Yen H (2002) Early salt stress effects on the changes in chemical composition in leaves of ice plant and Arabidopsis. A Fourier transforms infrared spectroscopy study. Plant Cell Physiol 130, 1032-1042.

Zhao D, Oosterhuis D (2002) Cotton carbon exchange, nonstructural carbohydrates, and

boron distribution in tissues during development of boron deficiency. Field Crop Res 78, 75-87.